The 2015 World Congress on
Advances in Civil, Environmental, and Materials Research (ACEM15)
Incheon, Korea, August 25-29, 2015

Analysis of Cracks in Isotropic Linear Elastic Half-space Under Various Boundary Conditions by Weakly Singular SGBEM

Tien Ngoc Pham[1)], *Jaroon Rungamornrat [1)], Withit Pansuk[1)] and Yasuhiko Sato[2)]

[1)] Department of Civil Engineering, Faculty of Engineering, Chulalongkorn University, Bangkok, Thailand 10330
[2)] Department of Civil Engineering, Faculty of Engineering, Hokkaido University, Sapporo, Japan 060-8628

ABSTRACT

In this paper, a weakly singular boundary integral equation method is established for the analysis of arbitrarily shaped cracks in an isotropic linear elastic half-space. Four different types of boundary conditions (BCs) on the surface of the half-space including the symmetric BC, the anti-symmetric BC, the traction-free BC, and the fully-fixed BC are treated. In the formulation, a pair of weakly singular, weak-form boundary integral equations for both the jump in the tractions and the sum of the displacement across the crack surface is employed to form a complete system of governing equations. This set of weakly singular integral equations can readily be obtained, for the first two BCs, by using a systematic regularization procedure proposed by Rungamornrat and Mear (2008a) along with the standard symmetrical and anti-symmetrical properties. For the last two BCs, they are obtained directly by applying a superposition technique to combine results of the first two BCs and the correction terms derived by Li (1996). To construct numerical solutions for the unknown jump and sum of the crack-face displacement, a weakly singular symmetric Galerkin boundary element method (SGBEM) is implemented. Besides an efficient scheme used to evaluate weakly singular and near singular double surface integrals resulting from the discretization, special crack-tip elements are also adopted along the crack front to enhance the accuracy of the approximation of the jump in the crack-face displacement near the crack front. Once the jump and the sum of the crack-face displacement are fully solved, they are used in the post-process to extract the stress intensity factors and T-stresses along the crack front. A selected set of results is then reported to demonstrate the accuracy, convergence, and robustness of the proposed numerical technique.

Keywords: Elastic half-space, SGBEM, Stress intensity factors, T-stresses, Weakly singular

*Corresponding Author, E-mail: jaroon.r@chula.ac.th

1. INTRODUCTION

Theoretical modeling of damages and flaws in various structural components, machine parts, and engineering devices has been found very crucial and commonly employed in the failure analysis and assessment which is considered an essential step in the design procedure. There are many situations encountered in practice where damages and flaws are induced relatively near the surface and their size is much smaller than the characteristic dimensions of the components. A half-space containing cracks supplied by a set of proper governing physics is one of mathematical models extensively employed and found sufficient for approximating those situations. To carry out such theoretical simulations, solution techniques have played an important role in the solution accuracy and computational performance and they must be properly selected to suit each involved scenario. Many investigations based on the conventional linear theory of fracture mechanics have been well recognized in the literature and various techniques including analytical methods, conventional domain-based numerical techniques, and boundary integral equation methods have been proposed to solve problems involving half-spaces containing cracks (e.g., Shah and Kobayashi, 1973; Lo, 1979; Murakami, 1985; Khai and Sushko, 1994; Sushko and Khai, 1996; Li, 1996; Hrylyts'kyi et al., 2003; Bogdanov, 2011; Gordeliy and Detournay, 2011).

For this particular boundary value problem, it is quite difficult to determine their solution using analytical approaches due to the complexity associated with general prescribed information such as crack geometries, boundary conditions, and loading conditions (Mayrhofer and Fischer, 1989). To broaden the modeling capability for cracked half-space problems, a variety of numerical procedures have continuously been developed. One of the favorite techniques based on the integral transforms was employed to derive the elastic fields and stress intensity factors for a penny-shaped crack in an isotropic elastic half-space (e.g., Srivastava and Singh, 1969; Feng et al., 2007; Bogdanov, 2011). Based on the fact that properties of the elastic fields are superposable, the body force method was proposed to estimate the stress intensity factors along the crack front of an elastic half-space containing planar cracks (e.g., Murakami, 1985; Noguchi and Smith, 1995; Noguchi et al., (1997)). Additionally, the cracked half-space problems were also solved by utilizing the alternating methods proposed by Smith and Alavi (1971) and Shah and Kobayashi (1973). Nonetheless, all the above studies were limited to certain crack configurations and the determination of stress intensity factors. The analysis for nonsingular terms was still not addressed.

Applications of boundary integral equation methods to the analysis of cracks in half-spaces have attracted several researchers. For instance, Lo (1979) established the governing boundary integral equations for an embedded planar crack in an elastic half-space; Khai and Sushko (1994) numerically investigated the influence of surface-coplanar cracks in a half-space with various geometrical dimensions; Sushko and Khai (1996) determined the functions characterizing the opening displacement of the surface-breaking crack during the deformation of a half-space; Khai and Sushko (1996) extended the work

of Khai and Sushko (1994) to treat cracks with the shape of Pascal (also see the work of Kit et al. (2000) and Hrylyts'kyi et al. (2003)). Additionally, Hayashi and Abé (1980) calculated the stress intensity factors of a semi-elliptical surface crack in a half-space using the collocation technique with a singular boundary integral equation. Another approach to establish a system of boundary integral equations for a normal crack in an elastic half-space was derived by Martin et al. (1993). Movchan and Willis (2000) extended the work of Martin et al. (1993) to treat a surface-breaking crack in a half-space. Among those works, the governing integral equations still contain Cauchy singular kernels and only mode-I stress intensity factors are evaluated for the special case of planar cracks. In recent years, Gordeliy and Detournay (2011) modeled arbitrarily shaped axisymmetric cracks in a homogeneous elastic half-space and whole space by using the displacement-discontinuity method. The governing hyper-singular integral equations established were then solved numerically by discretizing the crack into ring elements and utilizing the recursive relations for the element self-effect. Note in particular that this work only considered axisymmetric cracks and only the stress intensity factors were reported.

As previously mentioned, the boundary integral equation methods are computationally attractive for linear fracture analysis of cracked half-spaces. One of the advantages is that the key governing integral equations only requires discretization of surface rather than the whole domain of the problem and this significantly reduces the computational cost from that of the domain technique (e.g., Mayrhofer and Fischer, 1989; Hayashi and Abé, 1980; Kit et al., 2000). It can be remarked that the displacement integral equation derived directly from Somigliana's identity is insufficient for solving cracked bodies within the context of a single-domain formulation (e.g., Cruse, 1988). An alternative means to circumvent such difficult besides inefficient multi-domain techniques is to supply the traction boundary integral equation. Unfortunately, the conventional traction integral equation established directly from the stress integral relation contains both strongly singular and hyper-singular kernels and their treatment requires special care (e.g., Guiggiani et al., 1991). In addition, the smoothness requirement of the relative crack-face displacement data for the validity of the hyper-singular integral equation implies the need of using C^1-elements (e.g., Gray et al., 1990; Martin and Rizzo, 1996). To further alleviate such requirement and facilitate the integral treatment, a systematic regularization technique was proposed by Li (1996), Li and Mear (1998), and Li et al. (1998) to derive the singularity-reduced integral equations for discontinuities embedded in three-dimensional, isotropic, linear elastic unbounded, half-space, and finite media. This set of regularized integral equations were then utilized as a basis for the development of the weakly singular, symmetric Galerkin boundary element method for analysis of cracks in a whole space and finite bodies in the work of Li (1996) and Li et al. (1998). Nevertheless, on the basis of an extensive literature survey, the implementation of the integral equations derived by Li (1996) to treat cracks in an isotropic, elastic half-space has not been recognized.

In the present study, a numerical technique based on a weakly singular boundary integral equation method is established for the analysis of cracks in an isotropic linearly elastic half-space. The proposed work is carries out within a general framework allowing the treatment of arbitrary shaped cracks and half-spaces under various conditions on the

free surface and the determination of both stress intensity factors and the T-stresses along the crack front. Fundamental results constructed by Li (1996) are employed as the key ingredient along with symmetrical and anti-symmetrical features to form a set of governing boundary integral equations and the symmetric Galerkin boundary element scheme is then adopted to construct the approximate solutions. Remaining sections of this paper are organized to include the clear problem description, the formulation of the singularity-reduced boundary integral equations, the regularization procedure, the selected solution technique, results and discussion, and conclusions and remarks.

2. PROBLEM DESCRIPTION

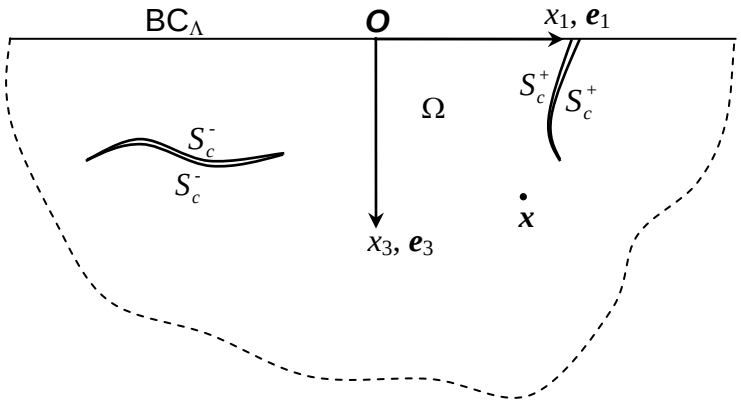

Fig. 1. Schematic of isotropic elastic half-space containing embedded and surface breaking cracks and subjected to boundary condition of the type BC$_\Lambda$ on the free surface

Let us consider a half-space Ω containing embedded and surface-breaking cracks as shown schematically in Fig. 1. For convenience in further development, a reference Cartesian coordinate system (***O***; x_1, x_2, x_3) with orthonormal base vectors {$\boldsymbol{e}_1$, $\boldsymbol{e}_2$, $\boldsymbol{e}_3$} is chosen such that the origin ***O*** is located on the free surface; the x_3-axis directs downward; the x_1- and x_2-axes follow the right hand rule; and $x_3 = 0$ presents the half-space surface. The body is made of a homogeneous, isotropic, linearly elastic material with shear modulus μ and Poisson's ratio ν. The cracks in the reference state can be represented by two geometrically identical surfaces S_c^+ and S_c^- with the corresponding outward unit normal vectors $\boldsymbol{n}^+$ and $\boldsymbol{n}^-$, respectively (see Fig. 1). On both crack surfaces S_c^+ and S_c^-, the pointwise self-equilibrated traction data is fully prescribed whereas, on the surface $x_3 = 0$, four types of boundary conditions, denoted by BC$_\Lambda$ for Λ = 1, 2, 3 and 4 (here and in what follows, the index Λ takes the value from 1 to 4 and the summation does not apply for the repeated Λ), are considered. For the symmetric boundary condition (BC), the normal component of the displacement and the shear tractions vanish identically (i.e.,

$u_3 = 0, \sigma_{13} = \sigma_{23} = 0$); for the anti-symmetric boundary condition (BC_2), tangential components of the displacement and the normal traction vanish (i.e., $u_1 = u_2 = 0, \sigma_{33} = 0$); for the traction-free boundary condition (BC_3), all components of the traction vanish (i.e., $\sigma_{13} = \sigma_{23} = \sigma_{33} = 0$); and for the fully-restrained boundary condition (BC_4), all components of the displacement vanish (i.e., $u_1 = u_2 = u_3 = 0$). In the present study, it is assumed that the body force and remote loading are absent. The key problem statement is to determine, in addition to the elastic field, the essential fracture data such as the relative crack-face displacement, the stress intensity factors, and T-stresses along the crack front.

3. STANDARD INTEGRAL RELATIONS

By applying the reciprocal theorem to the isotropic, linear elastic, half-space Ω containing cracks and subjected to crack-face loading and BC_Λ (Fig. 1) along with another elastic state associated with a fundamental problem of the uncracked half-space with the same boundary condition of BC_Λ and a unit concentrated force $\delta_{ip}\boldsymbol{e}_i$ at any interior point $\boldsymbol{x}$, it leads to a boundary integral relation for the displacement at point $\boldsymbol{x}$ of the cracked half-space

$$u_p^\Lambda(\boldsymbol{x}) = -\int_{S_c^+} S_{ij}^{\Lambda p}(\boldsymbol{\xi}, \boldsymbol{x}) n_i^+(\boldsymbol{\xi}) \Delta u_j^\Lambda(\boldsymbol{\xi}) dA(\boldsymbol{\xi}) \tag{1}$$

where $S_{ij}^{\Lambda p}(\boldsymbol{\xi}, \boldsymbol{x})$ denotes the stress fundamental solution of an uncracked half-space under BC_Λ and $\Delta u_j^\Lambda(\boldsymbol{\xi}) = u_j^{\Lambda+}(\boldsymbol{\xi}) - u_j^{\Lambda-}(\boldsymbol{\xi})$ denotes the jump in the displacements across the crack surfaces. After taking spatial derivative of (1) along with the use of a linear constitutive law for isotropic materials, a boundary integral relation for the stress at any interior point $\boldsymbol{x}$ of the cracked half-space under BC_Λ is given as

$$\sigma_{lk}^\Lambda(\boldsymbol{x}) = -\int_{S_c^+} E_{lkpq} \frac{\partial S_{ij}^{\Lambda p}(\boldsymbol{\xi}, \boldsymbol{x})}{\partial x_q} n_i^+(\boldsymbol{\xi}) \Delta u_j^\Lambda(\boldsymbol{\xi}) dA(\boldsymbol{\xi}) \tag{2}$$

where $E_{lkpq} = \mu[\delta_{lp}\delta_{kq} + \delta_{lq}\delta_{kp} + 2\nu\delta_{lk}\delta_{pq}/(1-2\nu)]$. While conventional boundary integral equations obtained directly by taking the limiting process of (1) and (2) to any point on the crack surface are sufficient for determining the crack-face unknown data (i.e., the displacement at each crack surface), it still requires nontrivial numerical treatment of singular integrals containing the strongly singular kernel $S_{ij}^{\Lambda p}(\boldsymbol{\xi}, \boldsymbol{x})$ and the hyper-singular kernel $E_{lkpq}\partial S_{ij}^{\Lambda p}(\boldsymbol{\xi}, \boldsymbol{x})/\partial x_q$.

4. SPECIAL DECOMPOSITIONS

To aid the regularization procedure of the boundary integral relations (1) and (2), the kernels $S_{ij}^{\Lambda p}(\boldsymbol{\xi},\boldsymbol{x})$ and $E_{lkpq}\partial S_{ij}^{\Lambda p}(\boldsymbol{\xi},\boldsymbol{x})/\partial x_q$ are decomposed into a form suiting the integration by parts via Stokes' theorem described in the next section. Such decompositions for all four types of boundary conditions can be obtained via the symmetrical/anti-symmetrical conditions and results established by Li (1996) and Rungamornrat and Mear (2008a).

4.1. Results for BC$_1$ and BC$_2$

Let us consider a half-space under the boundary condition BC$_\alpha$ (α = 1, 2); here and in what follows, the Greek index α takes the values 1 and 2. Based on the symmetrical and anti-symmetrical conditions, it can be seen that the half-space under BC$_\alpha$ subjected to a unit concentrated force $\delta_{ip}\boldsymbol{e}_i$ at a source point $\boldsymbol{x}=x_k\boldsymbol{e}_k$ as illustrated in Fig. 2(a) are identical to that of the bottom half of an elastic whole space subjected to a unit concentrated force $\Upsilon_\alpha\delta_{ip}\boldsymbol{e}_i$ (where $\Upsilon_1=\Upsilon_2=1$) acting at a point $\boldsymbol{x}=x_k\boldsymbol{e}_k$ and a unit concentrated force $\Pi_\alpha\overline{\delta}_{ip}\boldsymbol{e}_i$ (where $\Pi_1=1,\Pi_2=-1$ and $\overline{\delta}_{ip}$ is defined by $\overline{\delta}_{11}=\overline{\delta}_{22}=-\overline{\delta}_{33}=1$, $\overline{\delta}_{ij}=0$ for $i\neq j$) acting at a point $\overline{\boldsymbol{x}}=\overline{x}_k\boldsymbol{e}_k$ with $\overline{x}_k=\overline{\delta}_{kp}x_p$ as shown in Fig. 2(b). Upon using superimposition and results for the whole space, the stress fundamental solution $S_{ij}^{\alpha p}(\boldsymbol{\xi},\boldsymbol{x})$ can be obtained as

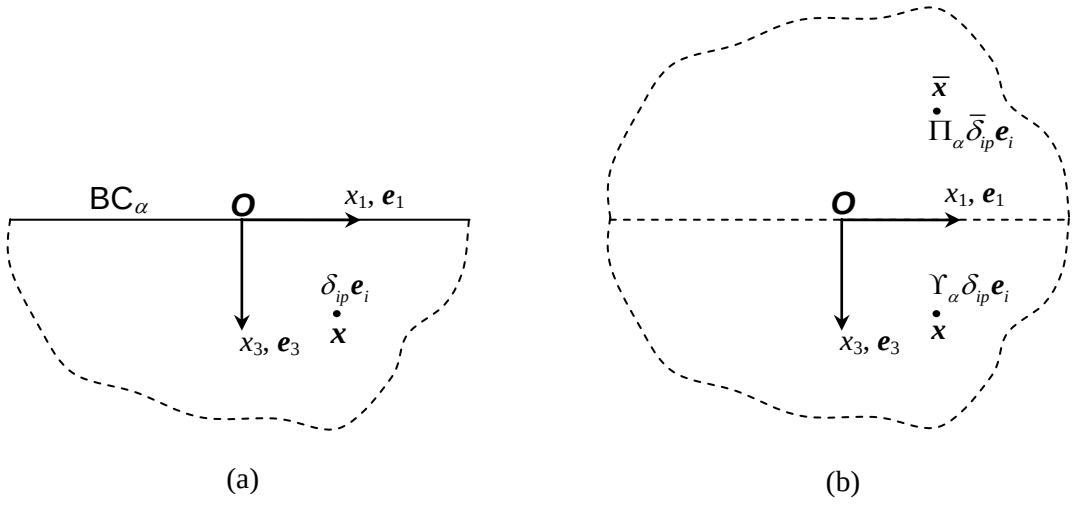

(a) (b)

Fig. 2. (a) Half-space under BC$_\alpha$ (α = 1, 2) and subjected to unit concentrated force $\delta_{ip}\boldsymbol{e}_i$ at point $\boldsymbol{x}$ and (b) whole space subjected to a pair of unit concentrated forces $\Upsilon_\alpha\delta_{ip}\boldsymbol{e}_i$ at a point $\boldsymbol{x}$ and $\Pi_\alpha\overline{\delta}_{ip}\boldsymbol{e}_i$ at its image point $\overline{\boldsymbol{x}}$

$$S_{ij}^{\alpha p}(\boldsymbol{\xi},\boldsymbol{x}) = \Upsilon_{\alpha} S_{ij}^{p}(\boldsymbol{\xi}-\boldsymbol{x}) + \Pi_{\alpha}\bar{\delta}_{pk} S_{ij}^{k}(\boldsymbol{\xi}-\bar{\boldsymbol{x}}) \tag{3}$$

where $S_{ij}^{p}(\boldsymbol{\xi}-\boldsymbol{x})$ denotes the stress fundamental solution for the whole space (see its explicit expression in Li, 1996). From properties of $S_{ij}^{p}(\boldsymbol{\xi}-\boldsymbol{x})$, the kernel $S_{ij}^{\alpha p}(\boldsymbol{\xi},\boldsymbol{x})$ is clearly singular only at $\boldsymbol{\xi}=\boldsymbol{x}$ of $\mathcal{O}(1/r^2)$. By using the relation (3), the kernel $E_{lkpq}\partial S_{ij}^{\alpha p}(\boldsymbol{\xi},\boldsymbol{x})/\partial x_q$ can be simplified to

$$E_{lkpq}\frac{\partial S_{ij}^{\alpha p}(\boldsymbol{\xi},\boldsymbol{x})}{\partial x_q} = -\Upsilon_{\alpha}\Sigma_{ij}^{lk}(\boldsymbol{\xi}-\boldsymbol{x}) - \Pi_{\alpha}\bar{\delta}_{ia}\bar{\delta}_{jb}\Sigma_{ab}^{lk}(\boldsymbol{x}-\bar{\boldsymbol{\xi}}) \tag{4}$$

where the kernel $\Sigma_{ij}^{lk}(\boldsymbol{\xi}-\boldsymbol{x})$ is defined by

$$\Sigma_{ij}^{lk}(\boldsymbol{\xi}-\boldsymbol{x}) = E_{lkpq}\frac{\partial S_{ij}^{p}(\boldsymbol{\xi}-\boldsymbol{x})}{\partial \xi_q} \tag{5}$$

Clearly, the kernel $E_{lkpq}\partial S_{ij}^{\alpha p}(\boldsymbol{\xi},\boldsymbol{x})/\partial x_q$ is singular only at $\boldsymbol{\xi}=\boldsymbol{x}$ of $\mathcal{O}(1/r^3)$. By employing special decompositions of the kernels $S_{ij}^{p}(\boldsymbol{\xi}-\boldsymbol{x})$ and $\Sigma_{ij}^{lk}(\boldsymbol{\xi}-\boldsymbol{x})$ proposed by Rungamornrat and Mear (2008a):

$$S_{ij}^{p}(\boldsymbol{\xi}-\boldsymbol{x}) = H_{ij}^{p}(\boldsymbol{\xi}-\boldsymbol{x}) + \varepsilon_{ism}\frac{\partial}{\partial \xi_s}G_{mj}^{p}(\boldsymbol{\xi}-\boldsymbol{x}) \tag{6}$$

$$E_{lkpq}\frac{\partial S_{ij}^{p}(\boldsymbol{\xi}-\mathbf{x})}{\partial \xi_q} = -E_{ijkl}\delta(\boldsymbol{\xi}-\boldsymbol{x}) + \varepsilon_{ism}\frac{\partial}{\partial \xi_s}\varepsilon_{lrt}\frac{\partial}{\partial \xi_r}C_{mj}^{tk}(\boldsymbol{\xi}-\boldsymbol{x}) \tag{7}$$

where ε_{ism} is a standard alternating symbol, $\delta(\boldsymbol{\xi}-\boldsymbol{x})$ is a Dirac-delta distribution centered at a point $\boldsymbol{x}$, and the functions $H_{ij}^{p}(\boldsymbol{\xi}-\boldsymbol{x})$, $G_{mj}^{p}(\boldsymbol{\xi}-\boldsymbol{x})$ and $C_{mj}^{tk}(\boldsymbol{\xi}-\boldsymbol{x})$ are defined by

$$H_{ij}^{p}(\boldsymbol{\xi}-\boldsymbol{x}) = -\delta_{jp}\frac{\xi_i - x_i}{4\pi r^3} \tag{8}$$

$$G_{mj}^{p}(\boldsymbol{\xi}-\boldsymbol{x}) = \frac{1}{8\pi(1-\nu)r}\left[(1-2\nu)\varepsilon_{mpj} + \varepsilon_{ijm}\frac{(\xi_i - x_i)(\xi_p - x_p)}{r^2}\right] \tag{9}$$

$$C_{mj}^{tk}(\boldsymbol{\xi}-\boldsymbol{x}) = \frac{\mu}{4\pi(1-\nu)r}\left[(1-\nu)\delta_{tk}\delta_{mj} + 2\nu\delta_{tj}\delta_{km} - \delta_{tm}\delta_{kj} - \delta_{tm}\frac{(\xi_k - x_k)(\xi_j - x_j)}{r^2}\right] \tag{10}$$

Both kernels $S_{ij}^{\alpha p}(\boldsymbol{\xi},\boldsymbol{x})$ and $E_{lkpq}\partial S_{ij}^{\alpha p}(\boldsymbol{\xi},\boldsymbol{x})/\partial x_q$ admit the decompositions

$$S_{ij}^{\alpha p}(\boldsymbol{\xi},\boldsymbol{x}) = H_{ij}^{\alpha p}(\boldsymbol{\xi},\boldsymbol{x}) + \varepsilon_{ism}\frac{\partial}{\partial \xi_s} G_{mj}^{\alpha p}(\boldsymbol{\xi},\boldsymbol{x}) \tag{11}$$

$$E_{lkpq}\frac{\partial S_{ij}^{\alpha p}(\boldsymbol{\xi},\boldsymbol{x})}{\partial x_q} = \Upsilon_\alpha E_{ijkl}\delta(\boldsymbol{\xi}-\boldsymbol{x}) - \Pi_\alpha \overline{\delta}_{ia}\overline{\delta}_{jb}E_{abkl}\delta(\boldsymbol{x}-\overline{\boldsymbol{\xi}}) + \varepsilon_{ism}\frac{\partial}{\partial \xi_s}\varepsilon_{lrt}\frac{\partial}{\partial x_r} C_{mj}^{\alpha tk}(\boldsymbol{\xi},\boldsymbol{x}) \tag{12}$$

where the functions $H_{ij}^{\alpha p}(\boldsymbol{\xi},\boldsymbol{x})$, $G_{mj}^{\alpha p}(\boldsymbol{\xi},\boldsymbol{x})$ and $C_{mj}^{\alpha tk}(\boldsymbol{\xi},\boldsymbol{x})$ are defined by

$$H_{ij}^{\alpha p}(\boldsymbol{\xi},\boldsymbol{x}) = \Upsilon_\alpha H_{ij}^{p}(\boldsymbol{\xi}-\boldsymbol{x}) + \Pi_\alpha \overline{\delta}_{pk} H_{ij}^{k}(\boldsymbol{\xi}-\overline{\boldsymbol{x}}) \tag{13}$$

$$G_{mj}^{\alpha p}(\boldsymbol{\xi},\boldsymbol{x}) = \Upsilon_\alpha G_{mj}^{p}(\boldsymbol{\xi}-\boldsymbol{x}) + \Pi_\alpha \overline{\delta}_{pk} G_{mj}^{k}(\boldsymbol{\xi}-\overline{\boldsymbol{x}}) \tag{14}$$

$$C_{mj}^{\alpha tk}(\boldsymbol{\xi},\boldsymbol{x}) = \Upsilon_\alpha C_{mj}^{tk}(\boldsymbol{\xi}-\boldsymbol{x}) - \Pi_\alpha \overline{\delta}_{am}\overline{\delta}_{bj} C_{ab}^{tk}(\boldsymbol{x}-\overline{\boldsymbol{\xi}}) \tag{15}$$

4.2. Results for BC_3 and BC_4

For an isotropic elastic half-space under BC_3 or BC_4, the decompositions of both $S_{ij}^{\Lambda p}(\boldsymbol{\xi},\boldsymbol{x})$ and $E_{lkpq}\partial S_{ij}^{\Lambda p}(\boldsymbol{\xi},\boldsymbol{x})/\partial x_q$ for $\Lambda = 3,4$ can be obtained by applying the linear superposition technique to combine results of BC_α and the correction terms derived by Li (1996). The final decompositions for BC_3 and BC_4 take the same form as (11) and (12) by simply replacing the superscript "α" by $\Lambda = 3,4$ and the following definition of the kernels

$$H_{ij}^{3p}(\boldsymbol{\xi},\boldsymbol{x}) = H_{ij}^{1p}(\boldsymbol{\xi},\boldsymbol{x}) \;\; ; \;\; H_{ij}^{4p}(\boldsymbol{\xi},\boldsymbol{x}) = H_{ij}^{2p}(\boldsymbol{\xi},\boldsymbol{x}) \tag{16}$$

$$G_{mj}^{3p}(\boldsymbol{\xi},\boldsymbol{x}) = G_{mj}^{1p}(\boldsymbol{\xi},\boldsymbol{x}) + \hat{G}_{mj}^{3p}(\boldsymbol{\xi},\boldsymbol{x}) \;\; ; \;\; G_{mj}^{4p}(\boldsymbol{\xi},\boldsymbol{x}) = G_{mj}^{2p}(\boldsymbol{\xi},\boldsymbol{x}) + \hat{G}_{mj}^{4p}(\boldsymbol{\xi},\boldsymbol{x}) \tag{17}$$

$$C_{mj}^{3tk}(\boldsymbol{\xi},\boldsymbol{x}) = C_{mj}^{1tk}(\boldsymbol{\xi},\boldsymbol{x}) + \hat{C}_{mj}^{3tk}(\boldsymbol{\xi},\boldsymbol{x}) \;\; ; \;\; C_{mj}^{4tk}(\boldsymbol{\xi},\boldsymbol{x}) = C_{mj}^{2tk}(\boldsymbol{\xi},\boldsymbol{x}) + \hat{C}_{mj}^{4tk}(\boldsymbol{\xi},\boldsymbol{x}) \tag{18}$$

where the explicit expression for $\hat{G}_{mj}^{3p}(\boldsymbol{\xi},\boldsymbol{x})$, $\hat{C}_{mj}^{3tk}(\boldsymbol{\xi},\boldsymbol{x})$, $\hat{G}_{mj}^{4p}(\boldsymbol{\xi},\boldsymbol{x})$ and $\hat{C}_{mj}^{4tk}(\boldsymbol{\xi},\boldsymbol{x})$ can be found in the work of Li (1996).

5. WEAKLY SINGULAR BOUNDARY INTEGRAL EQUATIONS

By using the decompositions (11) and (12) for both $S_{ij}^{\Lambda p}(\boldsymbol{\xi},\boldsymbol{x})$ and $E_{lkpq}\partial S_{ij}^{\Lambda p}(\boldsymbol{\xi},\boldsymbol{x})/\partial x_q$ with the index "α" being replaced by "Λ" and then integrating (1) and (2) by parts via Stokes' theorem, it leads to the singularity-reduced boundary integral relations

$$u_p^\Lambda(\boldsymbol{x}) = \int_{S_c^+} G_{mj}^{\Lambda p}(\boldsymbol{\xi},\boldsymbol{x}) D_m \Delta u_j^\Lambda(\boldsymbol{\xi}) dA(\boldsymbol{\xi}) - \int_{S_c^+} H_{ij}^{\Lambda p}(\boldsymbol{\xi},\boldsymbol{x}) n_i^+(\boldsymbol{\xi}) \Delta u_j^\Lambda(\boldsymbol{\xi}) dA(\boldsymbol{\xi}) \tag{19}$$

$$\sigma_{lk}^\Lambda(\boldsymbol{x}) = \varepsilon_{lrt}\frac{\partial}{\partial x_r}\int_{S_c^+} C_{mj}^{\Lambda tk}(\boldsymbol{\xi},\boldsymbol{x}) D_m \Delta u_j^\Lambda(\boldsymbol{\xi}) dA(\boldsymbol{\xi}) \tag{20}$$

where $D_m(\cdot) = n_i \varepsilon_{ism} \partial(\cdot)/\partial \xi_s$ denotes the surface differential operator. By further forming the limit of (19) and the product $\sigma_{lk}^{\Lambda}(\boldsymbol{x}) n_l^+(\boldsymbol{y})$ to point $\boldsymbol{y}$ on the crack surface, then constructing the weak-form statement, and finally integrating certain integrals by parts via Stokes' theorem, we obtain a pair of weak-form equations for the sum of the displacement and the jump in the traction across the crack surface as

$$\begin{aligned}\frac{1}{2}\int_{S_c^+} \tilde{t}_p(\boldsymbol{y}) \Sigma u_p^{\Lambda}(\boldsymbol{y}) dA(\boldsymbol{y}) = &-\int_{S_c^+} \tilde{t}_p(\boldsymbol{y}) \int_{S_c^+} H_{ij}^{\Lambda p}(\boldsymbol{\xi}, \boldsymbol{y}) n_i^+(\boldsymbol{\xi}) \Delta u_j^{\Lambda}(\boldsymbol{\xi}) dA(\boldsymbol{\xi}) dS(\boldsymbol{y}) \\ &+\int_{S_c^+} \tilde{t}_p(\boldsymbol{y}) \int_{S_c^+} G_{mj}^{\Lambda p}(\boldsymbol{\xi}, \boldsymbol{y}) D_m \Delta u_j^{\Lambda}(\boldsymbol{\xi}) dA(\boldsymbol{\xi}) dS(\boldsymbol{y})\end{aligned} \tag{21}$$

$$\frac{1}{2}\int_{S_c^+} \tilde{u}_k(\boldsymbol{y}) \Delta t_k^{\Lambda}(\boldsymbol{y}) dA(\boldsymbol{y}) = -\int_{S_c^+} D_t \tilde{u}_k(\boldsymbol{y}) \int_{S_c^+} C_{mj}^{\Lambda tk}(\boldsymbol{\xi}, \boldsymbol{y}) D_m \Delta u_j^{\Lambda}(\boldsymbol{\xi}) dA(\boldsymbol{\xi}) dA(\boldsymbol{y}) \tag{22}$$

where $\tilde{t}_p$ and $\tilde{u}_k$ are sufficiently smooth test functions; $\Sigma u_p^{\Lambda}(\boldsymbol{y}) = u_p^{\Lambda+}(\boldsymbol{y}) + u_p^{\Lambda-}(\boldsymbol{y})$ denotes the sum of the displacement across the crack surface; $\Delta t_k^{\Lambda}(\boldsymbol{y}) = t_k^{\Lambda+}(\boldsymbol{y}) + t_k^{\Lambda-}(\boldsymbol{y})$ denotes the jump in the traction across the crack surface. It is worth noting that the weak-form integral equations (21) and (22) contain only weakly singular kernels $H_{ij}^{\Lambda p}(\boldsymbol{\xi}, \boldsymbol{y}) n_i^+(\boldsymbol{\xi})$, $G_{mj}^{\Lambda p}(\boldsymbol{\xi}, \boldsymbol{y})$ and $C_{mj}^{\Lambda tk}(\boldsymbol{\xi}, \boldsymbol{y})$ of $\mathcal{O}(1/r)$.

6. SOLUTION PROCEDURE

The weakly singular weak-form boundary integral equation for the traction (22) is solved first for the unknown relative crack-face displacement Δu_j^{Λ} by a standard, weakly singular symmetric Galerkin boundary element method (SGBEM). Essential ingredients of this particular technique (e.g., discretization, evaluation of weakly singular and nearly singular double surface integration, linear solver, etc.) can be found in the work of Li et al. (1998) and Rungamornrat and Mear (2008b). It should also be emphasized that special crack-tip elements developed by Li et al. (1998) to integrate the square-type behavior are utilized not only to accurately approximate the relative crack-face displacement Δu_j^{Λ} in the vicinity of the crack front but also to allow the stress intensity factor to be extracted in a direct fashion in terms of the nodal degrees of freedom along the crack front. Once Δu_j^{Λ} is determined, the weak-form integral equation (21) is solved for the sum of the displacement on the crack surface using standard Galerkin technique. Standard isoparametric continuous elements are employed to approximate both Σu_p^{Λ} and $\tilde{t}_p$. Once the unknowns Δu_j^{Λ} and Σu_p^{Λ} on the crack surface are solved, the displacement and stress at any interior point of the half-space can be obtained from a pair of singularity-reduced boundary integral

relations (19) and (20). Besides the elastic field, the fracture information such as the stress intensity factors and the T-stresses are also of interest and can be extracted from the solved Δu_j^{Λ} and Σu_p^{Λ} following the similar procedures to those proposed by Li et al. (1998) and Subsathaphol (2013).

Let $\boldsymbol{x}_c$ be a point on the crack front and $\{\boldsymbol{x}_c; x_1, x_2, x_3\}$ be a local Cartesian coordinate system with the origin at $\boldsymbol{x}_c$ and the corresponding base vectors $\{\boldsymbol{e}_1, \boldsymbol{e}_2, \boldsymbol{e}_3\}$. In particular, the x_3-axis is tangent to the crack front; the x_1-axis directs outward and normal to the crack front such that x_1- x_3 plane forms a local tangent plane to the crack surface at $\boldsymbol{x}_c$; and x_2-axis follows the right hand rule as illustrated in Fig. 3. By using the property of special crack-tip elements, Li et al. (1998) derived an explicit formula for determining the mixed-mode stress intensity factors (K_I, K_{II}, K_{III}) in terms of extra nodal degrees of freedom along the crack front:

$$k_i(\boldsymbol{x}_c) = \sqrt{\frac{2\pi}{8}} \frac{1}{J_\eta \sin\beta} B_{il} f_l \tag{23}$$

where $\boldsymbol{x}_c$ denotes a generic nodal point on the crack front; $K_I = k_2$, $K_{II} = k_1$, $K_{III} = k_3$; $J_\eta = \| \partial \boldsymbol{r} / \partial \eta(\xi_c, -1) \|$; $\boldsymbol{r} = \boldsymbol{r}(\xi, \eta) = \boldsymbol{x}(\xi, \eta) - \boldsymbol{x}_c(\xi_c, -1)$; (ξ, η) are natural coordinates of any point $\boldsymbol{x}$ on the crack-tip element; $(\xi_c, -1)$ are natural coordinates of the nodal point $\boldsymbol{x}_c$; β is an angle between the unit vectors $\boldsymbol{e}_\eta$ and $\boldsymbol{e}_\xi$; $f_l = \hat{\boldsymbol{u}}(\boldsymbol{x}_c) \cdot \boldsymbol{e}_l$ with $\hat{\boldsymbol{u}}(\boldsymbol{x}_c)$ denoting the extra degree of freedom at $\boldsymbol{x}_c$; and $B_{il} = \mu/(1-\nu)[\delta_{i1}\delta_{l1} + \delta_{i2}\delta_{l2}] + \mu\delta_{i3}\delta_{l3}$. Once the stress intensity factors are determined at any nodal points, the value of those quantities at other points along the crack front can readily be obtained by using the interpolation technique.

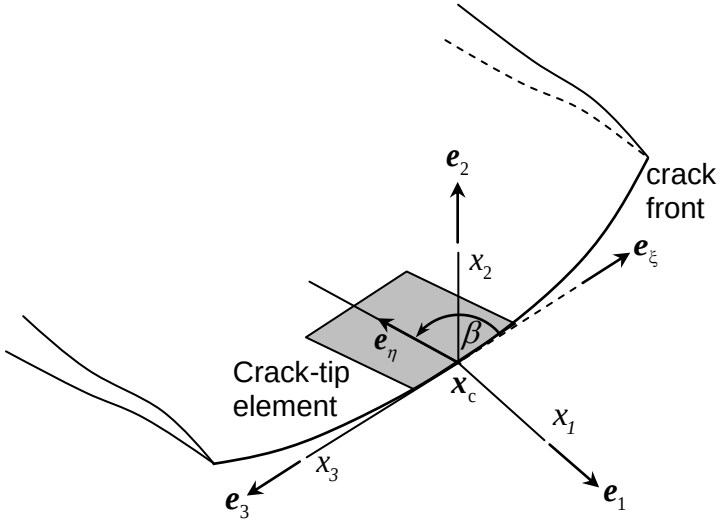

Fig. 3. Local Cartesian coordinate system and all involved parameters for determining stress intensity factors and T-stresses

The T-stresses along the crack front can also be extracted from the sum of the crack-face displacement as described below. The first non-singular stress tensor at the point $\boldsymbol{x}_c$, denoted by $T_{ij}(\boldsymbol{x}_c)$, can be related to the finite part of the strain tensor at the point $\boldsymbol{x}_c$, denoted by $\overline{\varepsilon}_{kl}(\boldsymbol{x}_c)$, via the following linear constitutive relation

$$T_{ij}(\boldsymbol{x}_c) = 2\mu\left[\overline{\varepsilon}_{ij}(\boldsymbol{x}_c) + \frac{\nu}{1-2\nu}\delta_{ij}\overline{\varepsilon}_{kk}(\boldsymbol{x}_c)\right] \tag{24}$$

It can readily be verified that the components T_{22}, T_{12} and T_{23} are known a priori and equal to the prescribed local traction on the crack surface at the point $\boldsymbol{x}_c$. The finite strain components $\overline{\varepsilon}_{11}$, $\overline{\varepsilon}_{33}$ and $\overline{\varepsilon}_{13}$ at the point $\boldsymbol{x}_c$ can be calculated from the sum of the crack-face displacement in the vicinity of the point $\mathbf{x}_c$ via the following relations

$$\overline{\varepsilon}_{11}(\boldsymbol{x}_c) = \frac{1}{2}\frac{\partial \Sigma u_1}{\partial x_1}(\boldsymbol{x}_c), \quad \overline{\varepsilon}_{33}(\boldsymbol{x}_c) = \frac{1}{2}\frac{\partial \Sigma u_3}{\partial x_3}(\boldsymbol{x}_c), \quad \overline{\varepsilon}_{13}(\boldsymbol{x}_c) = \frac{1}{4}\left(\frac{\partial \Sigma u_1}{\partial x_3}(\boldsymbol{x}_c) + \frac{\partial \Sigma u_3}{\partial x_1}(\boldsymbol{x}_c)\right) \tag{25}$$

The derivatives involved in the expressions (25) can be carried out directly within elements along the crack front. From the prescribed information of T_{22}, T_{12} and T_{23} and the computed strain components $\overline{\varepsilon}_{11}$, $\overline{\varepsilon}_{33}$ and $\overline{\varepsilon}_{13}$, the unknown components T_{11}, T_{13} and T_{33} at any point $\boldsymbol{x}_c$ along the crack front, commonly termed the T-stresses, can be obtained by solving a system of linear equations (24).

7. NUMERICAL RESULTS

A selected set of results is reported in this section to demonstrate the accuracy and capability of the proposed technique for all types of boundary conditions on the free surface. In the numerical study, Poisson's ratio is taken as ν = 0.3; a series of meshes with significantly different level of refinement are adopted to investigate the convergence behavior of numerical solutions; and 9-node crack-tip elements are employed along the crack front whereas 8-node quadrilateral and 6-node triangular elements are used for the remaining crack surface. The boundary integral formulation and numerical implementation are validated by benchmarking obtained results with available reference solutions.

7.1. Horizontal penny-shaped crack

Consider a penny-shaped crack embedded in a half-space with a depth *h* and the crack surface parallel to the free surface as shown in Fig. 4(a). The crack radius is denoted by *a* and the crack front is parameterized by $x_1 = a\cos\beta, x_2 = -a\sin\beta, x_3 = h$ for $\beta \in [0, 2\pi]$. The crack is subjected to uniform traction $t_1^+ = t_3^+ = \sigma_0, t_2^+ = 0$ (see Fig. 4(b)) and the free surface

of the half-space is under BC_1 or BC_2. In the analysis, three meshes are adopted as indicated in Fig. 4(d) and h/a = 0.5 is utilized.

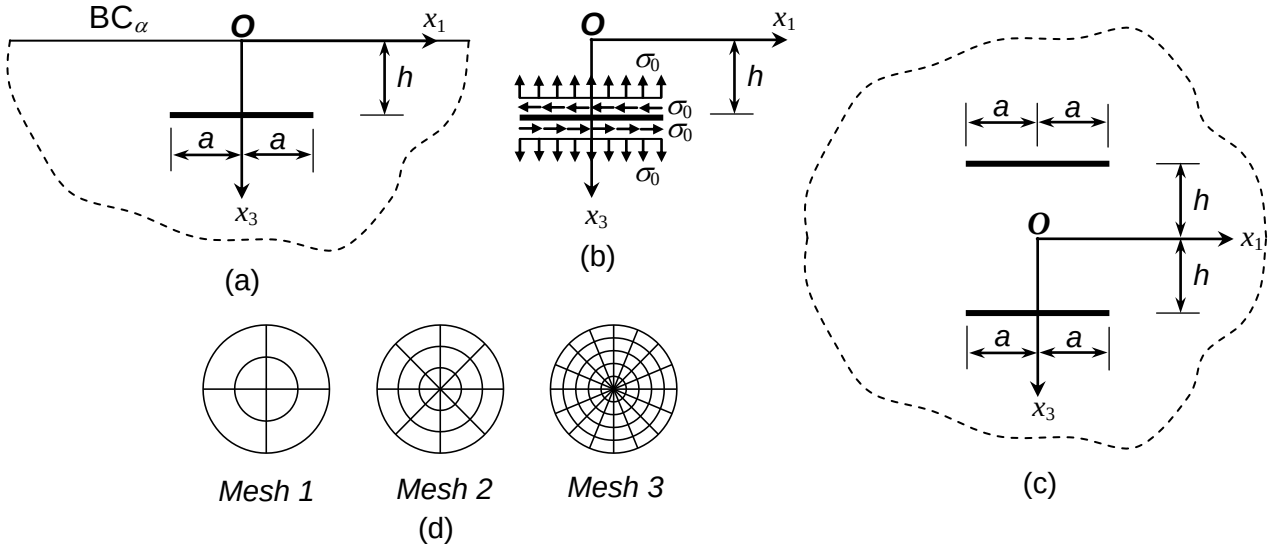

Fig. 4. (a) Schematic of horizontal penny-shaped crack embedded in half-space under BC_1 or BC_2, (b) tractions acting on crack surfaces, (c) equivalent problem associated with whole space, and (d) three meshes adopted in the analysis

Table 1
Normalized stress intensity factors at $\beta = \{0^0, 90^0, 180^0\}$ for horizontal penny-shaped crack embedded in half-space under BC_1 or BC_2 and h/a = 0.5

β	Mesh	BC_1			BC_2		
		K_I / K_I^{ref}	K_{II} / K_{II}^{ref}	K_{III} / K_{III}^{ref}	K_I / K_I^{ref}	K_{II} / K_{II}^{ref}	K_{III} / K_{III}^{ref}
0^0	1	0.9947	0.9894	-	0.9845	0.9805	-
	2	1.0002	0.9998	-	0.9987	0.9986	-
	3	1.0000	1.0000	-	1.0000	1.0000	-
90^0	1	0.9933	1.0007	0.9817	0.9861	0.9900	0.9945
	2	1.0000	1.0012	0.9989	0.9989	0.9997	1.0005
	3	1.0000	1.0000	1.0000	1.0000	1.0000	1.0000
180^0	1	0.9914	0.9909	-	0.9874	0.9761	-
	2	0.9997	1.0000	-	0.9990	0.9981	-
	3	1.0000	1.0000	-	1.0000	1.0000	-

Table 2
Normalized T-stresses at $\beta=\{0^0,90^0,180^0\}$ for horizontal penny-shaped crack embedded in half-space under BC_1 or BC_2 and *h*/*a* = 0.5

β	Mesh	BC_1			BC_2		
		T_{11}/T_{11}^{ref}	T_{33}/T_{33}^{ref}	T_{13}/T_{13}^{ref}	T_{11}/T_{11}^{ref}	T_{33}/T_{33}^{ref}	T_{13}/T_{13}^{ref}
0^0	1	1.0302	1.0202	-	0.9408	0.9646	-
	2	1.0130	1.0116	-	0.9713	0.9844	-
	3	1.0000	1.0000	-	1.0000	1.0000	-
90^0	1	1.0017	0.9980	0.9028	0.9925	0.9913	1.0520
	2	1.0021	1.0005	1.0832	0.9909	0.9974	1.0572
	3	1.0000	1.0000	1.0000	1.0000	1.0000	1.0000
180^0	1	0.9677	0.9655	-	1.0318	1.0107	-
	2	0.9893	0.9842	-	1.0057	1.0070	-
	3	1.0000	1.0000	-	1.0000	1.0000	-

The computed stress intensity factors and T-stresses at $\beta=\{0^0,90^0,180^0\}$ of both boundary conditions are normalized by the reference solution (generated from the whole space containing a pair of symmetrical cracks with respect to the surface $x_3=0$ shown in Fig. 4(c) and subjected to the symmetric loading condition for BC_1 and the anti-symmetric loading condition for BC_2 by using the Mesh 3) and reported in Table 1 and Table 2. As can be seen from results in Table 1, numerical solutions exhibit excellent agreement with the reference solution for all three meshes and their accuracy is weakly dependent on the level of mesh refinement. In particular, the percent different between results generated by the coarsest and intermediate meshes and the reference solution is less than 2% and 0.2% for the stress intensity factors and less than 6% and 3% for the T-stresses.

7.2. Vertical penny-shaped crack

Consider, next, a vertical penny-shaped crack of radius *a* embedded in a half-space with a depth *h* (measured from the center of the crack to the free surface) as shown in Fig. 5(a). The crack front is parameterized by $x_1=0, x_2=-a\cos\beta, x_3=h-a\sin\beta$ for $\beta\in[0,2\pi]$. The crack is subjected only to the uniform normal traction $t_1^+=\sigma_0, t_2^+=t_3^+=0$ (see Fig. 5(b)) and the free surface of the half-space is under all types of boundary conditions BC_Λ. In the analysis, three meshes of the penny-shaped crack are adopted as illustrated in Fig. 5(d) and *h*/*a* = 1.5 is considered.

For the first two boundary conditions BC_α, the computed stress intensity factors and T-stresses are normalized by the reference solution (generated from an equivalent whole space containing a pair of geometrically symmetric cracks with respect to the surface

$x_3 = 0$ shown in Fig. 5(c) and subjected to the symmetric loading condition for BC_1 and the anti-symmetric loading condition for BC_2 by using the Mesh 3) and reported in Table 3 and Table 4, respectively. Results of the stress intensity factors for the last two boundary conditions (i.e., BC_3 and BC_4) normalized by $K_I^{ref} = 2\sigma_0\sqrt{a/\pi}$ are compared with those obtained by Hrylyts'kyi et al. (2003) in Table 5. As indicated by results shown in Table 3, the stress intensity factors obtained from the three meshes for the first two boundary conditions are only slightly different from those obtained from the equivalent whole space problem. The discrepancy between the two solutions is small even though the coarsest mesh is utilized in the analysis. Similarly, the results in Table 4 suggest that the T-stresses obtained from the proposed technique for BC_1 and BC_2 agree very well with those obtained from the whole space problem with the percent difference less than 3.5% and 0.6% for Mesh 1 and Mesh 2, respectively. For BC_3 and BC_4, the numerical solutions for the mode-I stress intensity factors are in good agreement with those obtained by Hrylyts'kyi et al. (2003) and the dependence on the level of mesh refinement is insignificant. Only coarse meshes with few elements can be used to obtain reasonably accurate results. This high quality of the computed solutions is due primarily to the use of special crack-tip elements to capture the field in the neighborhood of the crack front.

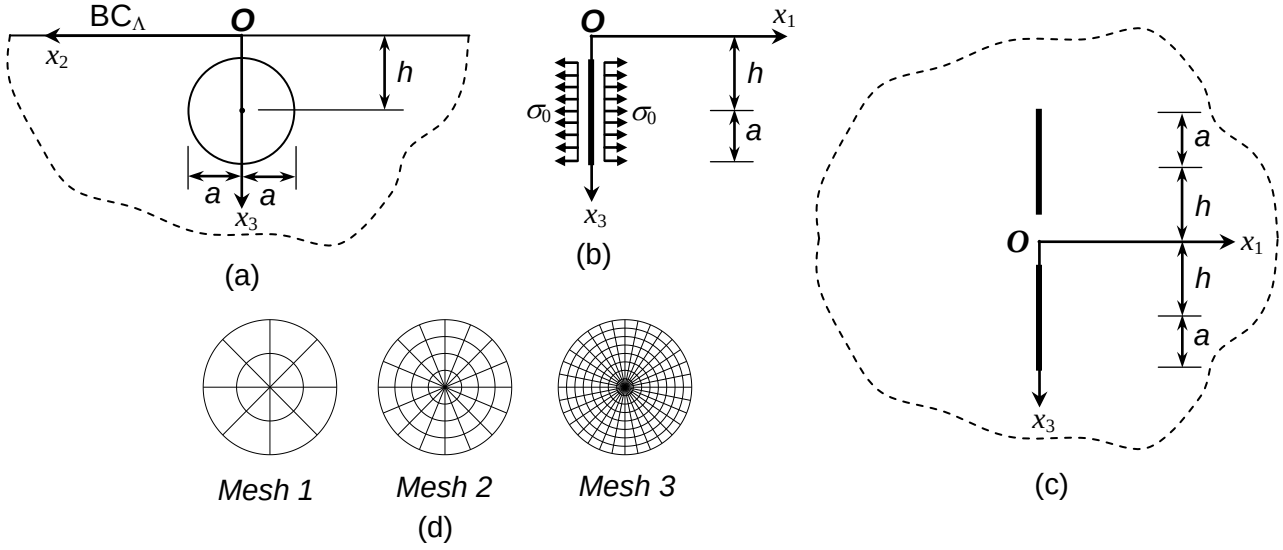

Fig. 5. (a) Schematic of vertical penny-shaped crack embedded in half-space under BC_Λ, (b) uniform normal traction acting to crack surfaces, (c) equivalent problem for BC_α associated with whole space, and (d) three meshes adopted in the analysis

Table 3
Normalized stress intensity factors at $\beta = \{0^0, 90^0\}$ for vertical penny-shaped crack embedded in half-space under BC_1 or BC_2 and *h*/*a* = 1.5

β	Mesh	BC_1	BC2
		K_I / K_I^{ref}	K_I / K_I^{ref}
0^0	1	0.9983	0.9984
	2	1.0000	1.0000
	3	1.0000	1.0000
90^0	1	0.9984	0.9983
	2	1.0000	1.0000
	3	1.0000	1.0000

Table 4
Normalized T-stresses at $\beta = \{0^0, 90^0\}$ for vertical penny-shaped crack embedded in half-space under BC_1 or BC_2 and *h*/*a* = 1.5

β	Mesh	BC_1			BC_2		
		T_{11} / T_{11}^{ref}	T_{33} / T_{33}^{ref}	T_{13} / T_{13}^{ref}	T_{11} / T_{11}^{ref}	T_{33} / T_{33}^{ref}	T_{13} / T_{13}^{ref}
0^0	1	1.0058	1.0018	1.0344	1.0056	1.0007	1.0323
	2	1.0022	1.0008	1.0057	1.0021	1.0005	1.0029
	3	1.0000	1.0000	1.0000	1.0000	1.0000	1.0000
90^0	1	1.0058	1.0020	-	1.0057	1.0004	-
	2	1.0024	1.0014	-	1.0018	0.9998	-
	3	1.0000	1.0000	-	1.0000	1.0000	-

Table 5
Normalized stress intensity factors at $\beta = \{0^0, 90^0\}$ for vertical penny-shaped crack embedded in half-space under BC_3 or BC_4 and *h*/*a* = 1.5. †Results obtained by means of extraction from certain figures reported by Hrylyts'kyi et al. (2003)

β	Mesh	Present results		Hrylyts'kyi	
		BC_3	BC_4	BC_3	BC_4
0^0	1	1.0195	0.9824	$1.0200^{\dagger}$	$0.9790^{\dagger}$
	2	1.0212	0.9839		
	3	1.0212	0.9840		
90^0	1	1.0510	0.9547	$1.0500^{\dagger}$	$0.9530^{\dagger}$
	2	1.0522	0.9565		
	3	1.0522	0.9566		

8. CONCLUSION AND REMARKS

A set of singularity-reduced boundary integral equations has been established for an isotropic, linearly elastic half-space containing arbitrary shaped cracks and subjected to various types of boundary conditions. The systematic regularization procedure proposed by Rungamornrat and Mear (2008a) along with results proposed by Li (1996) has been adopted to obtain the final completely regularized integral equations containing only weakly singular kernels. Another key feature of the developed integral equations is the automatic treatment of the free surface via the use of the fundamental solutions of the half-space with the same type of boundary conditions. This therefore avoids the discretization of the free surface in the solution procedure. A weakly singular symmetric Galerkin boundary element method has been implemented to numerically solve the weak-form traction boundary integral equation for the relative crack-face displacement and such information has then been used as the known data to determine the sum of the crack-face displacement from the weak-form displacement boundary integral equation by standard Galerkin technique. Special crack-tip elements have also been employed to enhance the approximation of the near-front field. The fracture data along the crack front such as the stress intensity factors and the T-stresses has been directly extracted from the relative and sum of crack-face displacement using the explicit formula.

Results from extensive numerical experiments and the comparison with several benchmarked cases have revealed that the proposed numerical procedure is highly accurate and computationally robust for the analysis of cracked half-spaces under various scenarios including arbitrary crack geometry, different boundary conditions and general loading conditions. Use of special crack-tip elements along the crack front has indicated that the stress intensity factors and T-stresses can be accurately captured using relatively very coarse meshes and this therefore renders the technique more suitable for linear fracture analysis than the standard finite element method which generally requires sufficiently fine mesh to capture the near-front field and experiences difficulty in treatment of an unbounded domain. While the proposed technique has been successfully implemented, it is still restricted to a half-space made of an isotropic linearly elastic material. The potential extension of the current work to treat a more general class of materials such as anisotropic solids and smart media is considered essential.

ACKNOWLEDGEMENTS

The authors are very grateful for the financial support from the JICA Project for AUN/SEED-Net Scholarship.

REFERENCES

Bogdanov, V. L. (2011), “Nonaxisymmetric problem of the stress-strain state of an elastic half-space with a near-surface circular crack under the action of loads along it.” *Journal of Mathematical Sciences*, Vol. **174**(3), 341-366.

Cruse, T. A. (1988), *Boundary Element Analysis in Computational Fracture Mechanics*, Kluwer Academic Publisher.

Feng, X. Q., Xu, M., Wang, X. and Gu, B. (2007), "Fracture mechanics analysis of three-dimensional ion cut technology." *Journal of Mechanics of Materials and Structures*, Vol. **2**(9), 1831-1852.

Gordeliy, E. and Detournay, E. (2011), "Displacement discontinuity method for modeling axisymmetric cracks in an elastic half-space." *International Journal of Solids and Structures*, Vol. **48**, 2614-2629.

Gray, L. J., Martha, L. F. and Ingraffea, A. R. (1990), "Hypersingular integrals in boundary element fracture analysis." *International Journal for Numerical Methods in Engineering*, Vol. **29**, 1135-1158.

Guiggiani, M., Krishnasamy, G., Rizzo, F. J. and Rudolphi, T. J. (1991), "Hypersingular boundary integral equations: A new approach to their numerical treatment." *Boundary Integral Method, Theory and Applications* (Edited by L. Morino, R. Piva and R. G. Piva), Springer-Velrag, Berlin, 211-220.

Hayashi, K. and Abé, H. (1980), "Stress intensity factors for a semi-elliptical crack in the surface of a semi-infinite solid." *Sijthoff & Noordhoff International Publishers Alphen aan den Rijn*, Vol. **16**(3), 275-285.

Hrylyts'kyi, M. D., Laushnyk, I. P. and Stankevych, O. M. (2003), "Reduction of the problem of interaction of cracks in a restrained half space to boundary integral equations." *Materials Science*, Vol. **39**(1), 79-85.

Khai, M. V. and Sushko, O. P. (1994), "Interaction of coplanar surface cracks in a half-space." *Strength of Materials*, Vol. **26**(10), 720-724.

Khai, M. V. and Sushko, O. P. (1996), "A study of the influence of the orientation of a planar surface crack in the shape of a limaçon of pascal on the stress concentration in a half-space." *Journal of Mathematical Sciences*, Vol. **81**(6), 3069-3072.

Kit, H.S., Khaj, M.V. and Sushko, O.P. (2000), "Investigation of the interaction of flat surface cracks in a half-space by BIEM." *International Journal of Engineering Science*, Vol. **38**, 1593-1616.

Li, S. (1996), *Singularity-reduced integral equations for discontinuities in three dimensional elastic media*, Ph.D. Dissertation, The University of Texas at Austin.

Li, S. and Mear, M. E. (1998), "Singularity-reduced integral equations for displacement discontinuities in three-dimensional linear elastic media." *International Journal of Fracture*, Vol. **93**, 87-114.

Li, S., Mear, M. E. and Xiao, L. (1998), "Symmetric weak-form integral equation method for three-dimensional fracture analysis." *Computer Methods in Applied Mechanics and Engineering*, Vol. **151**, 435-459.

Lo, K. K. (1979), "Three-dimensional crack in the interior of a half-space." *Sijthoff & Noordhoff International Publishers Alphen aan den Rijn*, Vol **9**(4), 435-439.

Martin, P. A., Päivärinta, L. and Rempel, S. (1993), "A normal crack in an elastic half-space with stress-free surface." *Mathematical Methods in the Applied Sciences*, Vol. **16**, 563-579.

Martin, P. A. and Rizzo, F. J. (1996), "Hypersingular integrals: how smooth must the density be?" *International Journal for Numerical Methods in Engineering*, Vol. **39**, 687-704.

Mayrhofer, K. and Fischer, F.D. (1989), "Stress intensity factor variation of a penny-shaped crack situated close to the free surface of a half-space." *7th International Conference on Fracture, Houston (USA)*, 83-89.

Movchan, N. V. and Willis, J. R. (2000), "Surface-breaking crack in an elastic half-space." *Journal of Engineering Mathematics, Kluwer Academic Publishers*, Vol. **37**, 143–154.

Murakami, Y. (1985), "Analysis of stress intensity factors of modes I, II and III for inclined surface cracks of arbitrary shape." *Engineering Fracture Mechanics*, Vol. **22**(1), 101-114.

Noguchi, H. and Smith, R. A. (1995), "An analysis of a semi-infinite solid with three-dimensional cracks." *Engineering Fracture Mechanics*, Vol. **52**(1), 1-14.

Noguchi, H., Smith, R. A., Carruthers, J. J. and Gilchrist, M. D. (1997), "Stress intensity factors of embedded elliptical cracks and an assessment of the ASME XI defect recharacterisation criteria." *International Journal of Pressure Vessels and Piping*, Vol. **70**, 69-76.

Rungamornrat, J. and Mear, M. E. (2008a), "Weakly-singular, weak-form integral equations for cracks in three-dimensional anisotropic media." *International Journal of Solids and Structures*,Vol. **45**, 1283-1301.

Rungamornrat, J. and Mear, M. E. (2008b), "A weakly-singular SGBEM for analysis of cracks in 3D anisotropic media." *Computer Methods in Applied Mechanics and Engineering*,Vol. **197**, 4319-4332.

Shah, R. C. and Kobayashi, A. S. (1973), "Stress intensity factors for an elliptical crack approaching the surface of a semi-infinite solid." *Noordhoff International Publishing-Leiden*, Vol. **9**(2), 133–146.

Smith, F. W. and Alavi, M. J. (1971), "Stress intensity factors for a penny shaped crack in a half space." *Engineering Fracfure Mechanics*, Vol. **3**, 241-254.

Srivastava, K. N. and Singh, K. (1969), "The effect of penny-shaped crack on the distribution of stress in a semi-infinite solid." *International Journal of Engineering Science*, Vol. **7**, 469-490.

Subsathaphol, T. (2013), *Analysis of T-stress for cracks in 3D linear piezoelectric media*, Master Thesis, Chulalongkorn University.

Sushko, O. P. and Khai, M. V. (1996), "Solution of problems of the theory of elasticity for a half-space with planar boundary cracks." *Journal of Mathematical Sciences*, Vol. **79**(6), 1434-1438.